



Supporting Online Material for

Recurrent Fusion of *TMPRSS2* and ETS Transcription Factor Genes in Prostate Cancer

Scott A. Tomlins, Daniel R. Rhodes, Sven Perner, Saravana M. Dhanasekaran, Rohit Mehra, Xiao-Wei Sun, Sooryanarayana Varambally, Xuhong Cao, Joelle Tchinda, Rainer Kuefer, Charles Lee, James E. Montie, Rajal B. Shah, Kenneth J. Pienta, Mark A. Rubin, Arul M. Chinnaiyan*

*To whom correspondence should be addressed. E-mail: arul@umich.edu

Published 28 October 2005, *Science* **310**, 644 (2005)
DOI: 10.1126/science.1117679

This PDF file includes:

Materials and Methods

Figs. S1 to S8

Tables S1 and S2

Supporting Online Material

Materials and Methods

Cancer Outlier Profile Analysis (COPA)

COPA analysis was performed on 132 gene expression data sets in OncoPrint 3.0 (www.oncoPrint.org) comprising 10,486 microarray experiments. COPA has three steps. First, gene expression values are median centered, setting each gene's median expression value to zero. Second, the median absolute deviation (MAD) is calculated and scaled to 1 by dividing each gene expression value by its MAD. Of note, median and MAD were used for transformation as opposed to mean and standard deviation so that outlier expression values do not unduly influence the distribution estimates, and are thus preserved post-normalization. Third, the 75th, 90th, and 95th percentiles of the transformed expression values are tabulated for each gene and then genes are rank-ordered by their percentile scores, providing a prioritized list of outlier profiles.

Samples

Tissues were from the radical prostatectomy series at the University of Michigan and from the Rapid Autopsy Program (*S1*), which are both part of University of Michigan Prostate Cancer Specialized Program of Research Excellence (S.P.O.R.E.) Tissue Core. Tissues were also obtained from a radical prostatectomy series at the University Hospital Ulm (Ulm, Germany). All samples were collected with informed consent of the patients and prior institutional review board approval at each institution. Total RNA from all samples was isolated with Trizol (Invitrogen, Carlsbad, CA) according to the manufacturer's instructions. Total RNA was also isolated from RWPE, PC3, PC3 cells stably transfected with the AR (PC3-AR) (*S2*), LNCaP, VCaP and DuCaP cell lines. VCaP and DuCaP cell lines were independently isolated from a vertebral and dural metastasis, respectively, from a patient with hormone-refractory prostate cancer (*S3,S4*). RNA integrity was verified by denaturing formaldehyde gel electrophoresis or the Agilent Bioanalyzer 2100 (Agilent Technologies, Palo Alto, CA). A commercially available pool of benign prostate tissue total RNA (CPP, Clontech, Mountain View, CA) was also used.

Quantitative PCR (QPCR)

Quantitative PCR (QPCR) was performed using SYBR Green dye on an Applied Biosystems 7300 Real Time PCR system (Applied Biosystems, Foster City, CA) (*S5, S6*). Briefly, 1-5 µg of total RNA was reverse transcribed into cDNA using SuperScript III (Invitrogen) in the presence of random primers or random primers and oligo dT primers. All reactions were performed with SYBR Green Master Mix (Applied Biosystems) and 25 ng of both the forward and reverse primer using the manufacturer's recommended thermocycling conditions. For each experiment, threshold levels were set during the exponential phase of the QPCR reaction using Sequence Detection Software version 1.2.2 (Applied Biosystems). The amount of each target gene relative to the housekeeping gene glyceraldehyde-3-phosphate dehydrogenase (*GAPDH*) for each sample was determined using the comparative threshold cycle (C_t) method (Applied Biosystems User Bulletin #2, <http://docs.appliedbiosystems.com/pebiiodocs/04303859.pdf>). For the experiments presented in Fig. 2, the relative amount of the target gene was calibrated to

the relative amount from a pool of benign prostate tissue (CPP). All oligonucleotide primers were synthesized by Integrated DNA Technologies (Coralville, IA). *GAPDH* (S7) and *PSA* (S8) primers were as described; all other primers are listed (**Table S2**). Approximately equal efficiencies of the primers were confirmed using serial dilutions of prostate cancer cDNA or plasmid templates in order to use the comparative G method. All reactions were subjected to melt curve analysis and products from selected experiments were resolved by electrophoresis on 1.5% agarose gels. As QPCR for *TMPRSS2:ERG* and *TMPRSS2:ETV1* resulted in measurable product after 35 cycles in some samples, melt curve analysis was used to reveal distinct amplicons, and products and primer-dimers could be resolved using gel electrophoresis.

RNA ligase mediated rapid amplification of cDNA ends (RLM-RACE)

RNA ligase mediated rapid amplification of cDNA ends was performed using the GeneRacer RLM-RACE kit (Invitrogen), according to the manufacturer's instructions. Initially, samples were selected based on expression of *ERG* or *ETV1* by QPCR. Five micrograms of total RNA was treated with calf intestinal phosphatase to remove 5' phosphates from truncated mRNA and non-mRNA and decapped with tobacco acid pyrophosphatase. The GeneRacer RNA Oligo was ligated to full length transcripts and reverse transcribed using SuperScript III. To obtain 5' ends, first-strand cDNA was amplified with Platinum Taq High Fidelity (Invitrogen) using the GeneRacer 5' Primer and *ETV1* exon 4-5_r for *ETV1* or the GeneRacer 5' Primer and *ERG* exon 4a_r or *ERG* exon 4b_r for *ERG*. The reverse primers were selected based on being in the 5'-most exons with over-expression in all tested samples. Primer sequences are given (**Table S2**). Products were resolved by electrophoresis on a 1.5% agarose gels and bands were excised, purified and TOPO TA cloned into pCR 4-TOPO. Purified plasmid DNA from at least 4 colonies was sequenced bi-directionally using M13 Reverse and M13 Forward (-20) primers or T3 and T7 primers on an ABI Model 3730 automated sequencer by the University of Michigan DNA Sequencing Core. RLM-RACEd cDNA was not used for the other assays.

Reverse-transcription PCR for TMPRSS2 fusion

After identifying *TMPRSS2:ERG* and *TMPRSS2:ETV1* positive cases using QPCR as described above, the same cDNA samples were PCR amplified with Platinum Taq High Fidelity and *TMPRSS2:ERG* and *TMPRSS2:ETV1* primers. Products were resolved by electrophoresis, cloned into pCR 4-TOPO and sequenced as described above. Additionally, cDNA samples were also PCR amplified with Platinum Taq High Fidelity using *TMPRSS2_RT-f* and *TMPRSS2:ERG_RT-r*. These products were resolved by electrophoresis and sequenced directly using the *TMPRSS2:ERG_RT* primers. cDNA samples were also amplified with Platinum Taq High Fidelity using *TMPRSS2_RT-f* and *TMPRSS2:ETV1_RT-r* and products were cloned into pCR4-TOPO and sequenced as described above.

In vitro androgen responsiveness

VCaP and LNCaP cells were grown in charcoal-stripped serum containing media for 24 hours. At 60% confluency, the cells were preincubated with bicalutamide dissolved in acetone (Casodex, AstraZeneca Pharmaceuticals, Wilmington, DE) and flutamide

dissolved in ethanol (Sigma, St. Louis, MO) at a final concentration of 10 μ M. After 2 hours 0.5nM of the synthetic androgen methyltrienolone (R1881, NEN Life Science Products, Boston, MA) dissolved in ethanol was added and the cells were harvested after 48 hours. For the experiment presented in **Fig. S8**, DuCaP, RWPE, PC3 and PC3+AR cells were grown in charcoal-stripped serum containing media for 24 hours before treatment for 48 hours with 1% vehicle or 1 nM R1881. Total RNA was isolated and subjected to reverse transcription and QPCR as described above with ERG exon 5-6_f and _r primers.

Fluorescence in situ hybridization (FISH)

Formalin-fixed paraffin-embedded (FFPE) tissue sections from normal peripheral lymphocytes and the metastatic prostate cancer samples MET-26 and MET-28 were used for interphase FISH. In addition we also performed interphase FISH on a tissue microarray containing cores from FFPE sections of 13 clinically localized prostate cancer and 16 metastatic prostate cancer samples. For metaphase FISH on VCaP cells, metaphase spreads were prepared using standard methods. We employed a two-color, two-signal approach to evaluate the fusion of *TMPRSS2* and *ETV1*, with probes spanning most of the respective gene loci. The biotin-14-dCTP BAC clone RP11-124L22 was used for the *ETV1* locus and the digoxin-dUTP labeled BAC clone RP11-35C4 was used for the *TMPRSS2* locus. For analyzing gene rearrangements involving ERG, we utilized a split-signal probe strategy, with two probes spanning the ERG locus (digoxin-dUTP labeled BAC clone RP11-95I21, (5') and biotin-14-dCTP labeled BAC clone RP11-476D17 (3')). For metaphase samples, the above probes for *TMPRSS2* and the 5' ERG region were used together. All BAC clones were obtained from the Children's Hospital of Oakland Research Institute (CHORI). Prior to tissue analysis, the integrity and purity of all probes were verified by hybridization to metaphase spreads of normal peripheral lymphocytes. Although the 5' ERG clone produced weak, but reproducible signals on chromosome 2 from metaphases, these signals could easily be distinguished from the much stronger target signals on interphase studies. Tissue hybridization, washing and color detection were performed as described (S6, S9). For evaluation of the interphase FISH on the TMA, an average of 108 cells per case were evaluated for assessment of *TMPRSS2:ETV1* and 115 cells per case for the ERG rearrangement. For *TMPRSS2:ETV1* positive cases, an average of 31% of cells had the fusion. For ERG rearrangement positive cases, an average of 79.7% of cells had the rearrangement.

Southern Hybridization

Genomic DNA (10 μ g) from VCaP, RWPE and PC3 cells was digested with EcoRI overnight. Fragments were resolved on a 0.8% agarose gel at 40 V overnight, transferred to Hybond NX nylon membrane, prehybridized, hybridized with probe and washed according to standard protocols. The probe was prepared by PCR amplification with Platinum Taq High Fidelity on normal male genomic DNA using primers for a 497 bp product between exons 1 and 2 of *TMPRSS2*, and 25 ng was labeled with dCTP-P³² and used for hybridization. Primers were: forward, 5'-GCTCCAGGCCATATGTGAACTTTCTAAT-3'; reverse, 5'-GATAAGATGCCACACCCAGACAAC.

Supporting Figures

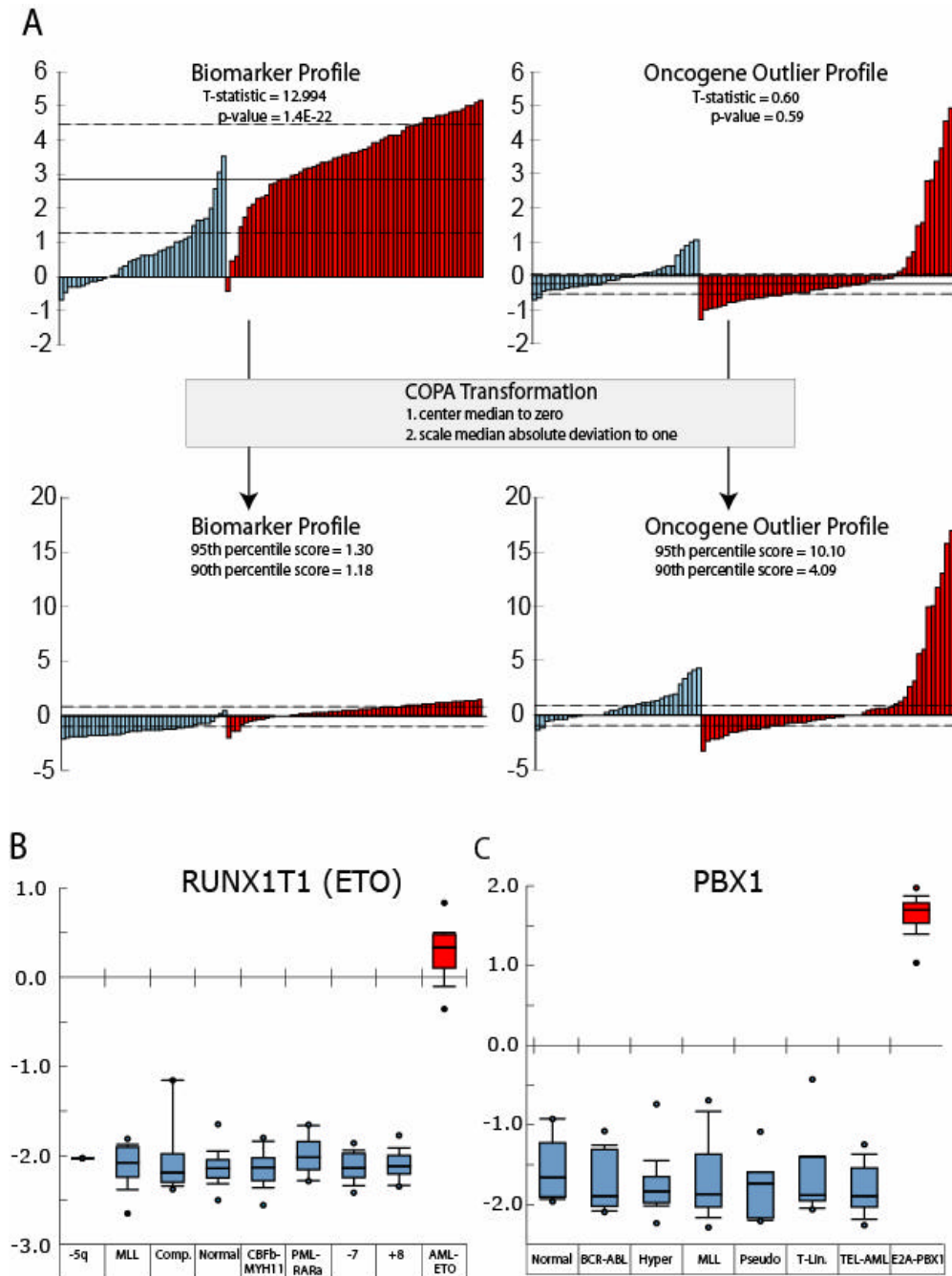


Figure S1. Cancer Outlier Profile Analysis (COPA).

(A) COPA schematic. A hypothetical biomarker profile is characterized by general over-expression in cancer (red) relative to normal tissue (blue), whereas a hypothetical oncogene outlier profile is characterized by general low expression with marked over-expression in a fraction of cancer samples. Statistical tests such as Student's t-test are powerful for identifying genes with biomarker profiles, but not genes with outlier profiles, as evidenced by the respective t-statistics and p-values. The COPA

transformation centers the median expression value to zero (solid line) and scales the median absolute deviation (dashed line) to one, so to dampen biomarker-type profiles and accentuate outlier-type profiles. The final step in COPA is the tabulation and rank-ordering of percentile scores from the post-transformation values. **(B)** *RUNX1T1 (ETO)* had the highest scoring outlier profile at the 90th percentile in the Valk *et al.* acute myeloid leukemia dataset (n = 293) (*S10*). The outlier profile correctly associated with the documented *AML-ETO* translocation. Sample classes are indicated as defined by Valk *et al.* based on pertinent features of the karyotype: -5(q) abnormalities, 11q23 rearrangements of *MLL*, complex karyotype (greater than three chromosomal abnormalities), normal karyotype, inv (16) resulting in *CBFb-MYH11*, t(15;17) resulting in *PML-RAR α* , -7(q) abnormalities, +8 abnormalities and t(8;21) resulting in *AML-ETO*. **(C)** *PBX1* had the highest scoring outlier profile in the Ross *et al.* acute lymphoblastic leukemia dataset (n = 132) (*S11*). Again the outlier profile perfectly associated with the documented *E2A-PBX1* translocation. Sample classes are indicated as defined by Ross *et al.* based on pertinent features of the karyotype: normal karyotype, t(9;21) resulting in *BCR-ABL*, hyperdiploid (>50 chromosomes), 11q23 rearrangements of *MLL*, pseudodiploid, T cell lineage ALL, t(12;21) resulting in *TEL-AML* and t(1;19) resulting in *E2A-PBX1*.

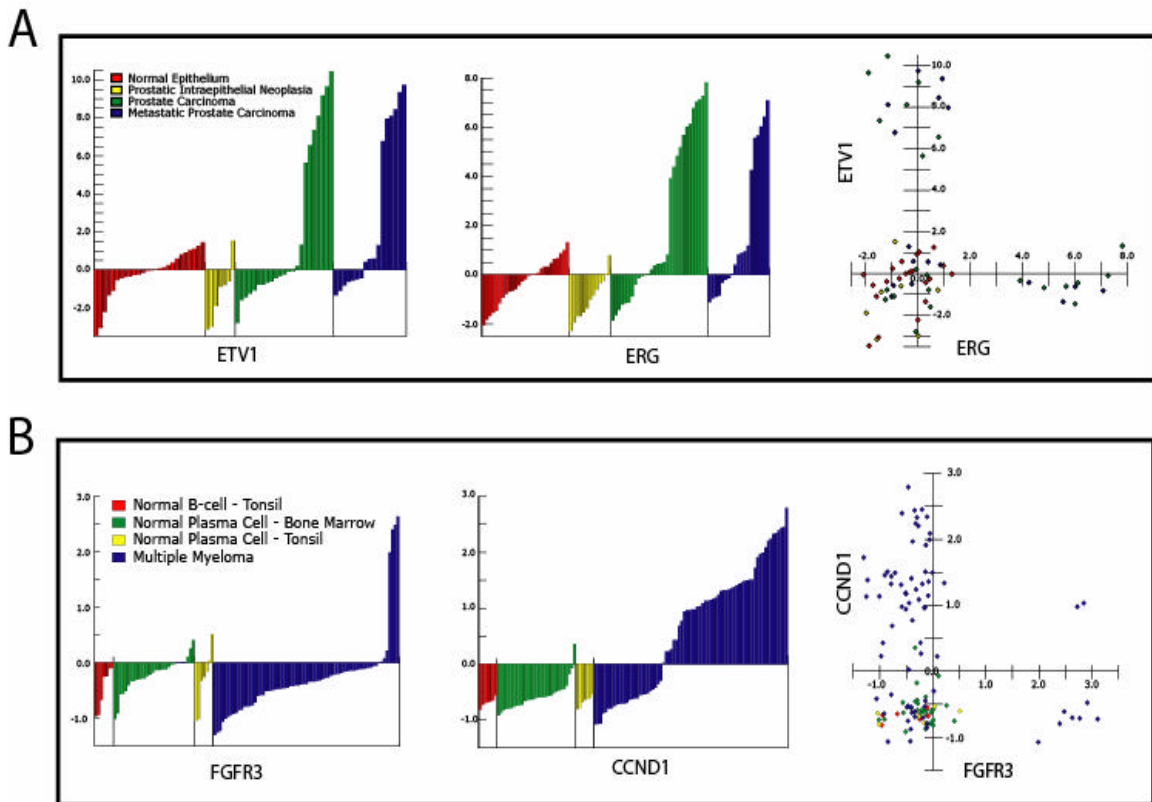


Figure S2. Exclusive outlier expression of *ERG* and *ETV1* is consistent with other fusions involving multiple partner genes. **(A)** *ETV1* and *ERG* expression (normalized expression units) are shown from 101 profiled samples isolated by laser capture microdissection. Visualization tools incorporated in OncoPrint V3.0 (www.oncoPrint.org) were used to generate graphical displays. Sample classes are indicated according to the color scale. Scatter plots of *ERG* and *ETV1* expression across all of the profiled samples are shown (right panels). **(B)** As in **(A)** except oncogenes (*FGFR3* and *CCND1*) with known fusion to the immunoglobulin heavy chain promoter (*IgH*) in multiple myeloma were examined from (S12).

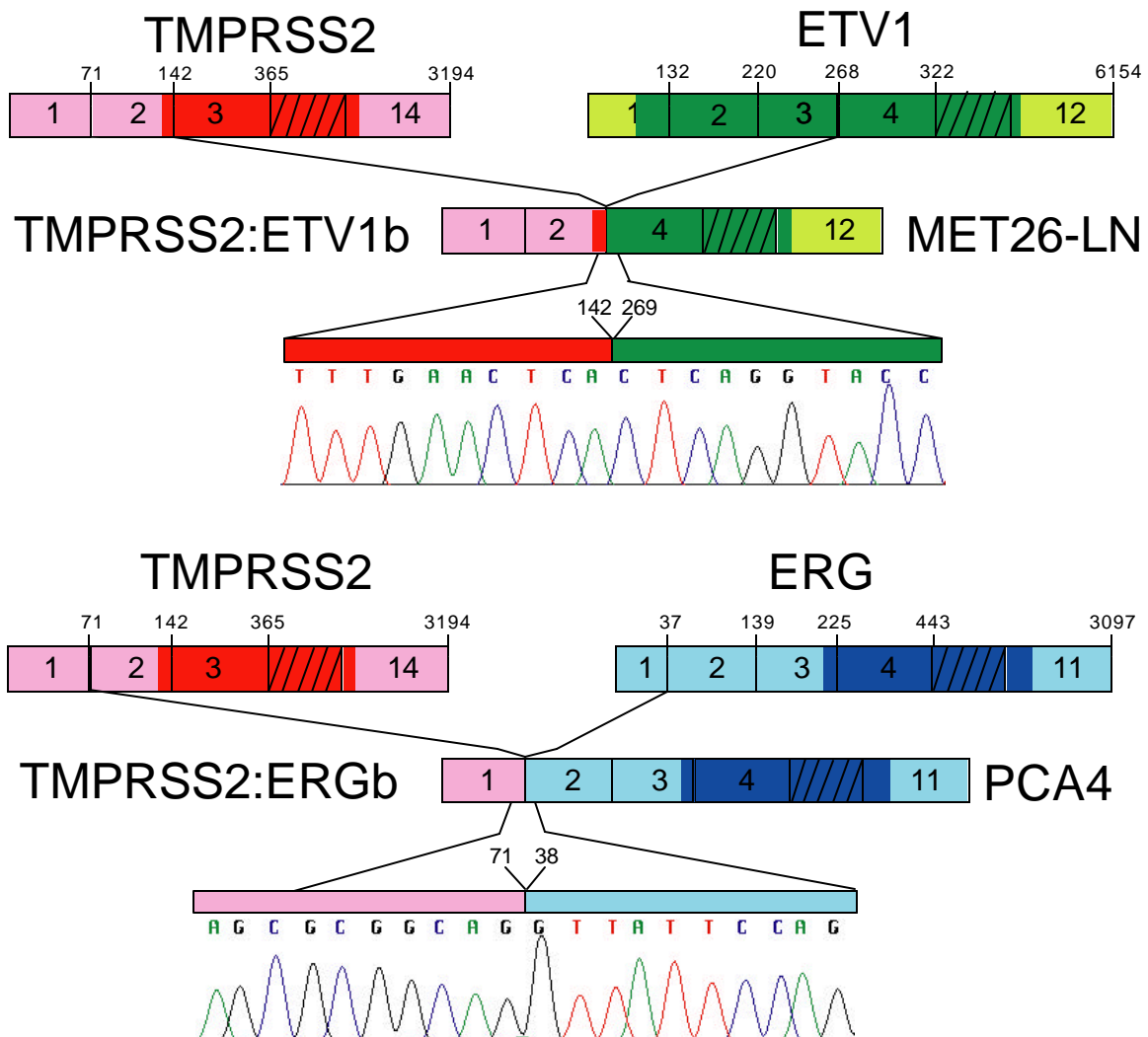


Figure S3. Schematic of RNA ligase-mediated rapid amplification of cDNA ends (RLM-RACE) results revealing fusions of *TMPRSS2* with *ETV1* in MET26-LN and *ERG* in PCA4. Gene structures for *TMPRSS2*, *ERG* and *ETV1* are shown using the GenBank reference sequences (NM_005656.2, NM_004449.3, and NM_004956.3, respectively). Exons (indicated by boxes) for *TMPRSS2* (shades of red), *ERG* (shades of blue) and *ETV1* (shades of green) are numbered according to alignment of the reference sequence with the May 2004 assembly of the human genome using the UCSC Genome browser. Numbers above the exons indicate the last base of each exon. Untranslated regions according to the reference sequences are shown in corresponding lighter shades of color. Coding exons not depicted are indicated by the hashed boxes. Identified fusions of *TMPRSS2:ETV1b* in MET26-LN and *TMPRSS2:ERGb* in PCA4 are indicated, with exon color and numbering from the original reference sequences. Insets show the position and automated DNA sequencing of the fusion points.

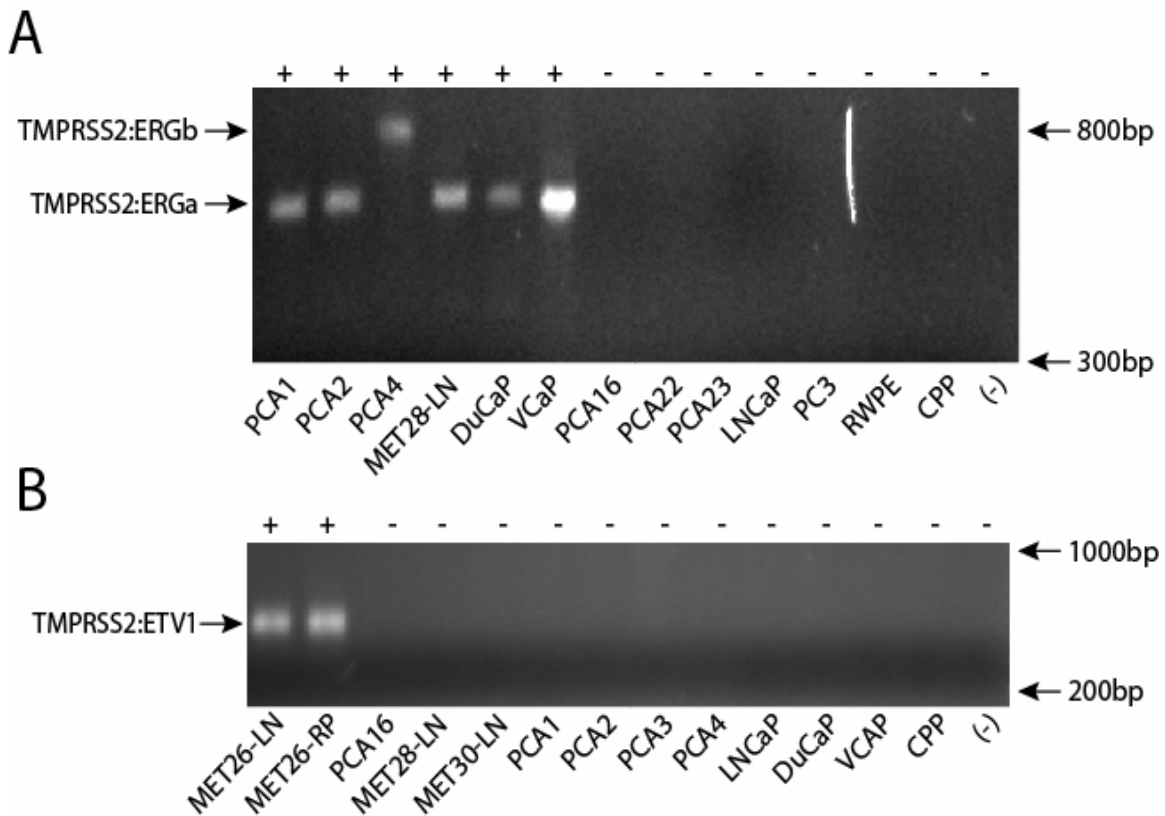


Figure S4. Reverse-transcribed cDNA from localized (PCA) and metastatic (MET) prostate cancer samples or prostate cancer cell lines expressing *TMPRSS2:ERG* or *TMPRSS2:ETV1* by QPCR (indicated by + or – above the sample) was amplified by PCR with forward primers in exon 1 of *TMPRSS2* and reverse primers in exon 6 of *ERG* or exon 7 of *ETV1*. The expected sizes of *TMPRSS2:ERG* and *TMPRSS2:ETV1* are indicated. No template control reactions (-) were also included.

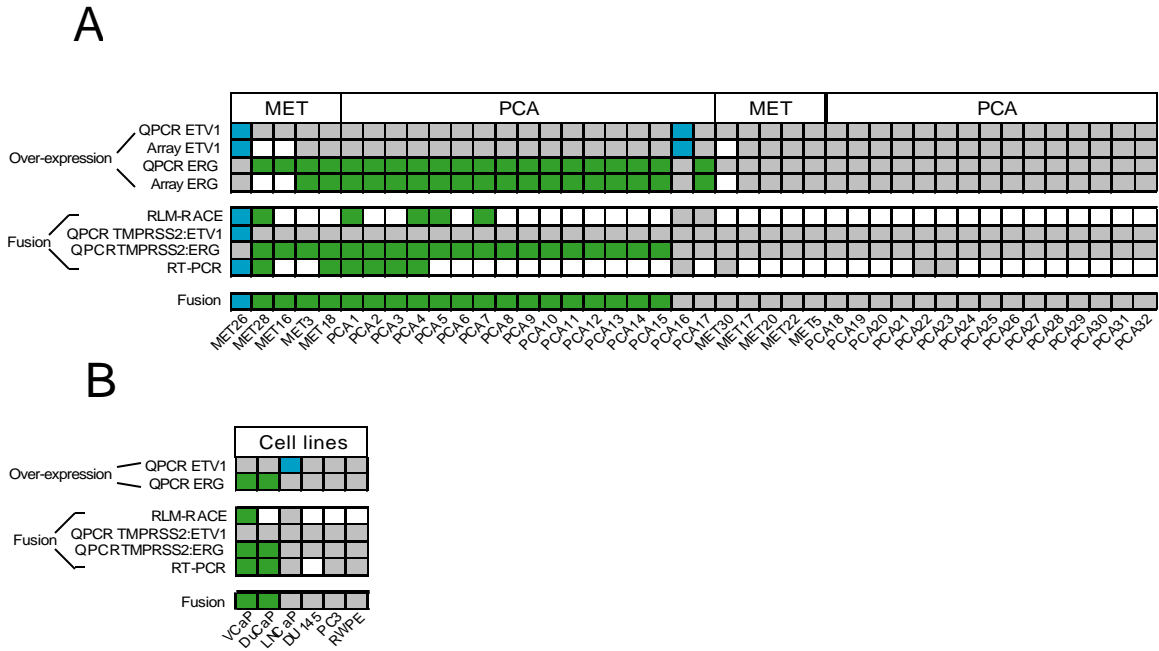


Figure S5. Summary of *TMPRSS2* fusion to ETS family member status in prostate cancer samples and cell lines. **(A)** Rows represent individual assays and columns represent metastatic (MET) or localized prostate cancer (PCA) samples as indicated. For all assays, positive results are indicated by colored cells, negative results are indicated by grey cells. Blank cells indicate that assay was not performed for that sample. Over-expression of *ETV1* (blue cells) or *ERG* (green cells) by QPCR and cDNA microarray is indicated in the upper panel. Assays for fusion of *TMPRSS2* with *ETV1* (blue cells) or *ERG* (green cells) are indicated, including RLM-RACE for the over-expressed ETS family member, QPCR for *TMPRSS2:ETV1* and *TMPRSS2:ERG* expression, and sequencing of reverse-transcription PCR (RT-PCR) products. Samples with evidence for *TMPRSS2:ETV1* or *TMPRSS2:ERG* fusion are indicated in the final row. **(B)** As in **(A)**, except columns represent prostate cell lines.

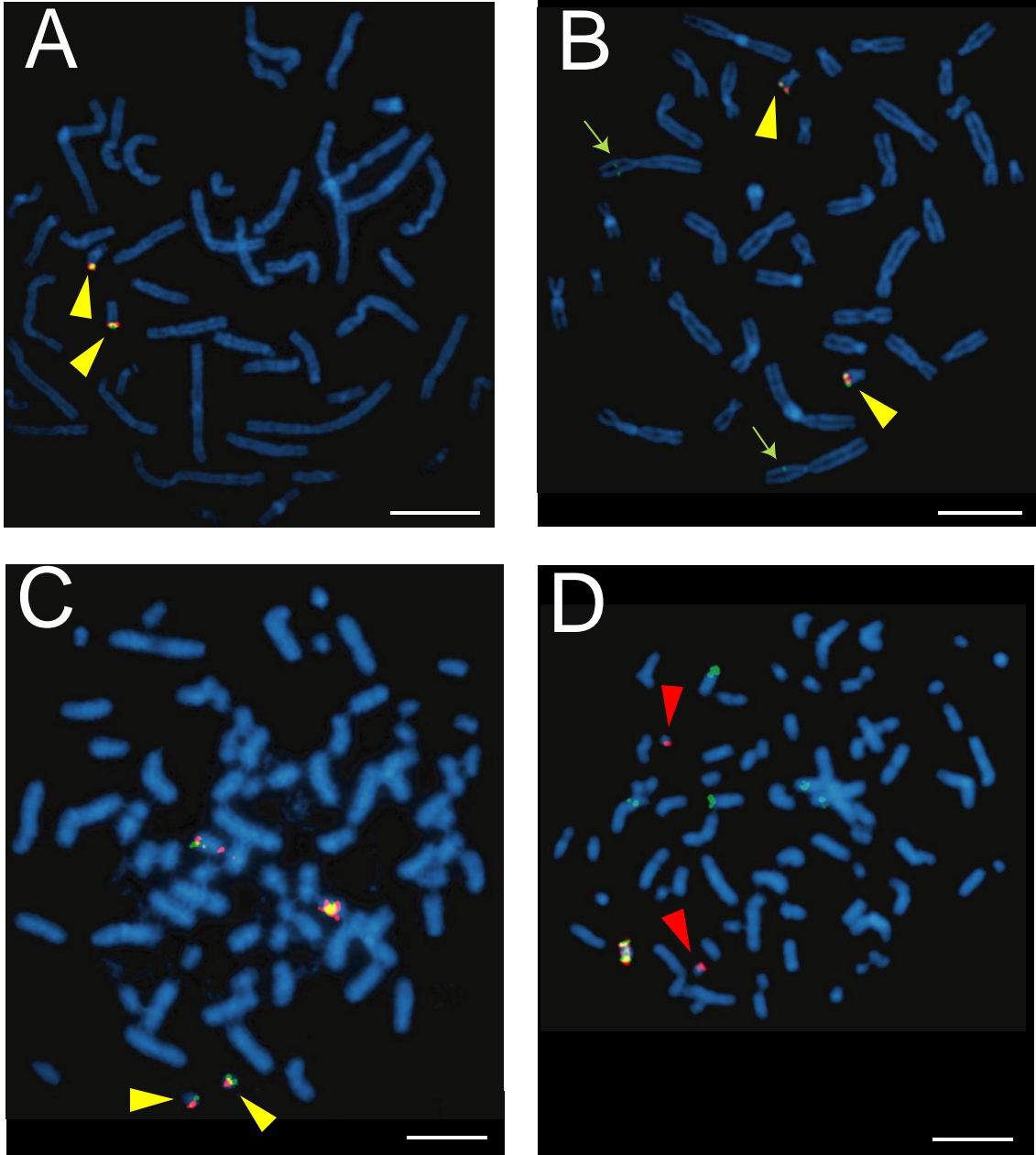


Figure S6. Metaphase FISH confirms rearrangement of *ERG* in VCaP prostate cancer cells. **(A)** Due to the proximity of *ERG* and *TMPRSS2* on chromosome 21 (~3 megabases), probes for *TMPRSS2* (green) and 3' *ERG* (red) appear colocalized (yellow arrowheads) in normal peripheral lymphocytes (NPLs). **(B)** Co-localization (yellow arrowheads) of 5' (green) and 3' *ERG* (red) probes in NPLs. Reproducible signals from the 5' *ERG* probe of weak intensity were also visible on chromosome 2 (green arrows). **(C and D)** Using the same set of probes on VCaP metaphases, *TMPRSS2* signals remain juxtaposed to *ERG* 3' signals (**C**, yellow arrowheads), while co-localization of 5' and 3' *ERG* signals is lost (**D**, red arrowheads). For all the images the scale bar is 10 μm .

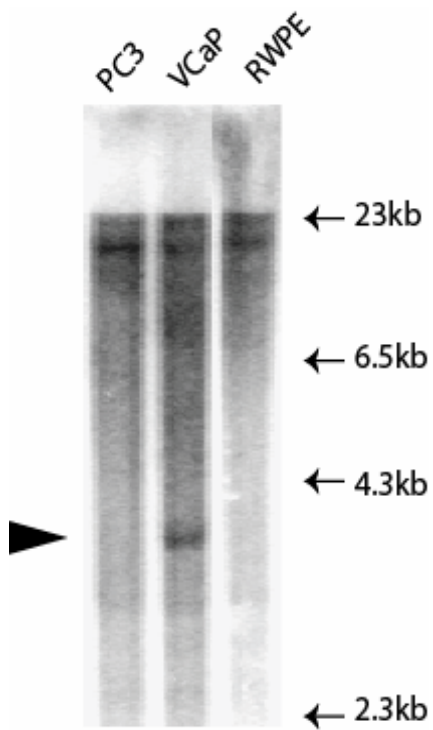


Figure S7. Southern blotting confirms rearrangement of *TMPRSS2* in VCaP prostate cancer cells. Genomic DNA (10 μ g) from RWPE, VCaP and PC3 cells were digested using EcoRI. A probe from genomic DNA in the intron between *TMPRSS2* exons 1 and 2 detects an additional band (arrowhead) in VCaP cells, which express the *TMPRSS2:ERG* fusion.

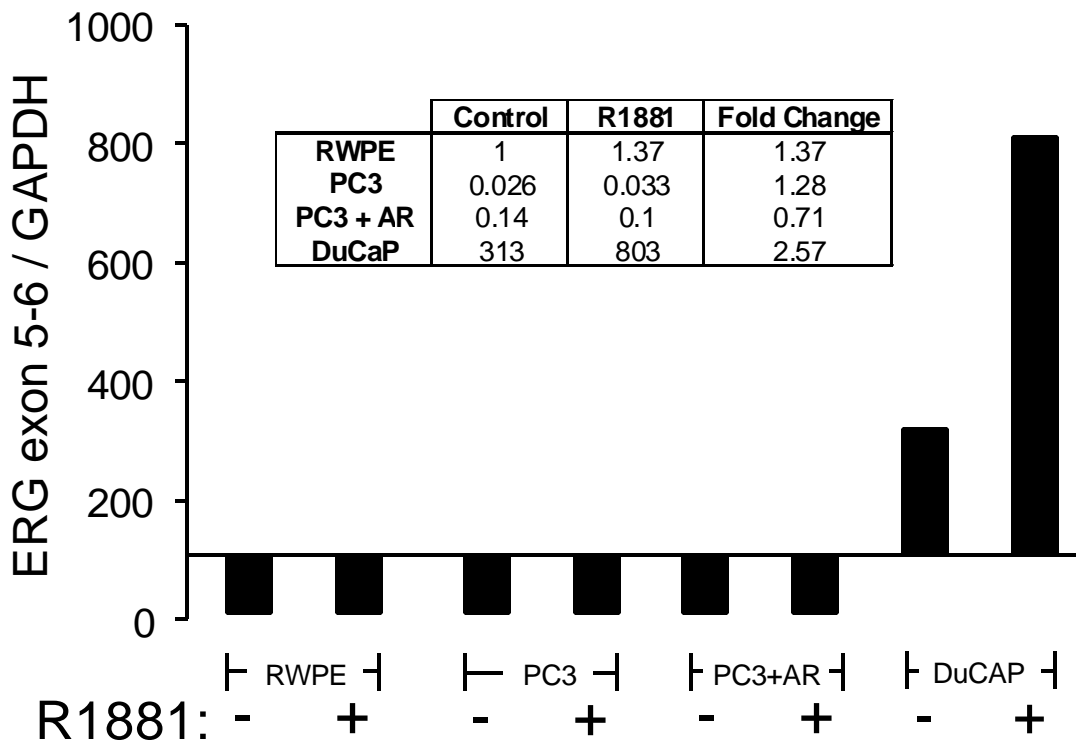


Figure S8. Androgen regulation of *ERG* in DuCaP cells, which express *TMPRSS2:ERG*. *ERG* (exon 5-6) expression in androgen sensitive immortalized benign prostate cells (RWPE), androgen sensitive prostate cancer cell lines (DuCaP), the androgen insensitive prostate cancer cell line (PC3) and PC3 cells transfected with the human androgen receptor (PC3-AR) was assessed by QPCR. Cell lines were treated for 48 hours with 1% vehicle or 1nM of the synthetic androgen R1881. *ERG/GAPDH* is reported with all samples normalized to the RWPE control sample and the fold change of *ERG* expression upon androgen stimulation is given in the inset.

Supporting Tables

Table S1. Cancer Outlier Profile Analysis (COPA). Genes that are known to undergo causal mutations in cancer that had an outlier profile in the top 10 of a study in OncoPrint are shown. “X”, signifies literature evidence for acquired pathognomonic translocation. “XX” signifies that samples in the specific study were characterized for the indicated translocation. “Y” signifies consistent with known amplification. “***” signifies ERG and ETV1 outlier profiles in prostate cancer.

Rank	%	Score	Gene	Cancer	Study	Reference	Evidence
1	90	21.9346	<i>CDH1</i>	Melanoma	Bittner et al.	(S13)	
1	95	20.056	<i>RUNX1T1</i>	Leukemia	Valk et al.	(S10)	XX
1	95	15.4462	<i>PRO1073</i>	Renal	Vasselli et al.	(S14)	X (S15)
1	95	14.2008	<i>MYH11</i>	Sarcoma	Segal et al.	(S16)	
1	90	12.9581	<i>PBX1</i>	Leukemia	Ross et al.	(S11)	XX
1	95	10.03795	<i>ETV1</i>	Prostate	Lapointe et al.	(S17)	**
1	90	7.4557	<i>WHSC1</i>	Myeloma	Tian et al.	(S18)	X (S19)
1	75	5.4071	<i>ERG</i>	Prostate	Dhanasekaran et al.	(S20)	**
1	75	5.2067	<i>FOXO3A</i>	Breast	Wang et al.	(S21)	
1	75	4.3628	<i>ERG</i>	Prostate	Welsh et al.	(S22)	**
1	75	4.3425	<i>CCND1</i>	Myeloma	Zhan et al.	(S12)	X (S23)
1	75	3.724	<i>PCSK7</i>	Leukemia	Cheok et al.	(S24)	
1	75	3.4414	<i>ERG</i>	Prostate	Lapointe et al.	(S17)	**
1	75	3.3875	<i>ERG</i>	Prostate	Dhanasekaran et al.	(S25)	**
1	75	2.5913	<i>IGH@</i>	Lung	Wigle et al.	(S26)	
2	90	12.7953	<i>HOXA9</i>	Leukemia	Ross et al.	(S11)	
2	95	9.2916	<i>TRA@</i>	Leukemia	Golub et al.	(S27)	
2	95	9.2916	<i>TRD@</i>	Leukemia	Golub et al.	(S27)	
2	90	8.2292	<i>SSX2</i>	Leukemia	Cheok et al.	(S24)	
3	95	13.3478	<i>FGFR3</i>	Myeloma	Zhan et al.	(S12)	X (S23)
3	95	10.2267	<i>ARHGAP26</i>	Leukemia	Cheok et al.	(S24)	
3	75	2.6162	<i>TCL1A</i>	Lymphoma	Rosenwald et al.	(S28)	
3	75	2.036	<i>RAD51L1</i>	Breast	Sotiriou et al.	(S29)	
4	75	8.4985	<i>TP53</i>	Melanoma	Bittner et al.	(S13)	
4	90	5.4881	<i>LCK</i>	Leukemia	Golub et al.	(S27)	
4	75	2.5728	<i>ERBB2</i>	Breast	Huang et al.	(S30)	Y (S31)
4	75	2.0229	<i>IGL@</i>	Ovarian	Schwartz et al.	(S32)	
6	90	17.3733	<i>ZBTB16</i>	Leukemia	Ferrando et al.	(S33)	
6	95	9.1267	<i>FGFR2</i>	Gastric	Chen et al.	(S34)	
6	90	6.6079	<i>ERBB2</i>	Breast	Sotiriou et al.	(S29)	Y (S31)
6	75	5.7213	<i>NF1</i>	Prostate	LaTulippe et al.	(S35)	
6	75	5.2752	<i>PHOX2B</i>	Endocrine	Jain et al.	(S36)	
6	90	4.8383	<i>LAF4</i>	Prostate	Lapointe et al.	(S17)	
6	90	4.1779	<i>IRTA1</i>	Lymphoma	Alizadeh et al.	(S37)	
6	90	3.6325	<i>IRTA1</i>	Lymphoma	Rosenwald et al.	(S38)	
6	75	1.85865	<i>HMGA1</i>	Liver	Chen et al.	(S39)	
7	95	4.7561	<i>NONO</i>	Colon	Alon et al.	(S40)	
7	75	1.8133	<i>GPC3</i>	Liver	Chen et al.	(S39)	
8	90	4.7068	<i>EVI1</i>	Leukemia	Lacayo et al.	(S41)	
8	90	4.7068	<i>MDS1</i>	Leukemia	Lacayo et al.	(S41)	
9	95	17.1698	<i>ETV1</i>	Prostate	Glinsky et al.	(S42)	**
9	90	15.3889	<i>MN1</i>	Leukemia	Ferrando et al.	(S33)	
9	90	6.60865	<i>SSX1</i>	Sarcoma	Nielsen et al.	(S43)	X (S44)
9	90	4.4875	<i>CHEK2</i>	Prostate	Lapointe et al.	(S17)	
9	75	2.2218	<i>ERG</i>	Prostate	Yu et al.	(S45)	**
10	95	10.6036	<i>KIT</i>	Sarcoma	Segal et al.	(S16)	

Table S2. Oligonucleotide primers used in this study. For all primers, the gene, bases and exons (according to alignment of the reference sequences for *TMPRSS2*, *ERG* and *ETV1*, (NM_005656.2, NM_004449.3, and NM_004956.3 respectively) with the May 2004 assembly of the human genome using the UCSC Genome Browser) are listed. Forward primers are indicated with “f” and reverse primers with “r”.

Gene	Bases	Exon(s)	Primer	Sequence 5' to 3'
ETV1	193-216	2	Exon 2-3_f	AACAGAGATCTGGCTCATGATTCA
ETV1	268-245	3	Exon 2-3_r	CTTCTGCAAGCCATGTTTCCTGTA
ETV1	248-271	3-4	Exon 3-4_f	AGGAAACATGGCTTGCAGAAGCTC
ETV1	305-280	4	Exon 3-4_r	TCTGGTACAAACTGCTCATCATTGTC
ETV1	269-294	4	Exon 4-5_f	CTCAGGTACCTGACAATGATGAGCAG
ETV1	374-351	5	Exon 4-5_r	CATGGACTGTGGGGTTCTTTCTTG
ETV1	404-429	5	Exon 5-6_f	AACAGCCCTTTAAATTCAGCTATGGA
ETV1	492-472	6	Exon 5-6_r	GGAGGGCCTCATTCCCCTTG
ETV1	624-645	6-7	Exon 6-7_f	CTACCCCATGGACCACAGATTT
ETV1	771-750	7	Exon 6-7_r	CTTAAAGCCTTGTGGTGGGAAG
ERG	574-597	5-6	Exon 5-6_f	CGCAGAGTTATCGTGCCAGCAGAT
ERG	659-636	6	Exon 5-6_r	CCATATTCTTT CACCGCCCACTCC
NA	NA	NA	Generacer 5'_f	CGACTGGAGCACGAGGACACTGA
ETV1	374-351	5	Exon 4-5_r	CATGGACTGTGGGGTTCTTTCTTG
ERG	284-263	4	Exon 4a_r	GGCGTTCCGTAGGCACACTCAA
ERG	396-377	4	Exon 4b_r	CCTGGCTGGGGTTGAGACA
TMPRSS2	-4 - 17	1	TMPRSS2:ERG_f	TAGGCGCGAGCTAAGCAGGAG
ERG	276-252	4	TMPRSS2:ERG_r	GTAGGCACACTCAAACAACGACTGG
TMPRSS2	1-19	1	TMPRSS2:ETV1_f	CGCGAGCTAAGCAGGAGGC
ETV1	339-318	4-5	TMPRSS2:ETV1_r	CAGGCCATGAAAAGCCAAACTT
TMPRSS2	12-28	1	TMPRSS2_RT-f	CAGGAGGCGGAGGCGGA
ERG	762-742	6	TMPRSS2:ERG_RT-r	GGCGTTGTAGCTGGGGGTGAG
ETV1	762-741	7	TMPRSS2:ETV1_RT-r	TTGTGGTGGGAAGGGGATGTTT

References and Notes

- S1. R. B. Shah *et al.*, *Cancer Res* **64**, 9209 (2004).
- S2. J. L. Dai, C. A. Maiorino, P. J. Gkonos, K. L. Burnstein, *Steroids* **61**, 531 (1996).
- S3. S. Korenchuk *et al.*, *In Vivo* **15**, 163 (2001).
- S4. Y. G. Lee *et al.*, *In Vivo* **15**, 157 (2001).
- S5. P. Chinnaiyan *et al.*, *Cancer Res* **65**, 3328 (2005).
- S6. M. A. Rubin *et al.*, *Cancer Res* **64**, 3814 (2004).
- S7. J. Vandesompele *et al.*, *Genome Biol* **3**, RESEARCH0034 (2002).
- S8. K. Specht *et al.*, *Am J Pathol* **158**, 419 (2001).
- S9. L. A. Garraway *et al.*, *Nature* **436**, 117 (2005).
- S10. P. J. Valk *et al.*, *N Engl J Med* **350**, 1617 (2004).
- S11. M. E. Ross *et al.*, *Blood* **102**, 2951 (2003).
- S12. F. Zhan *et al.*, *Blood* **99**, 1745 (2002).
- S13. M. Bittner *et al.*, *Nature* **406**, 536 (2000).
- S14. J. R. Vasselli *et al.*, *Proc Natl Acad Sci U S A* **100**, 6958 (2003).
- S15. I. J. Davis *et al.*, *Proc Natl Acad Sci U S A* **100**, 6051 (2003).
- S16. N. H. Segal *et al.*, *J Clin Oncol* **21**, 1775 (2003).
- S17. J. Lapointe *et al.*, *Proc Natl Acad Sci U S A* **101**, 811 (2004).
- S18. E. Tian *et al.*, *N Engl J Med* **349**, 2483 (2003).
- S19. J. J. Keats *et al.*, *Blood* **105**, 4060 (2005).
- S20. S. M. Dhanasekaran *et al.*, *Faseb J* **19**, 243 (2005).
- S21. Y. Wang *et al.*, *Lancet* **365**, 671 (2005).
- S22. J. B. Welsh *et al.*, *Cancer Res* **61**, 5974 (2001).
- S23. R. Fonseca *et al.*, *Cancer Res* **64**, 1546 (2004).
- S24. M. H. Cheok *et al.*, *Nat Genet* **34**, 85 (2003).
- S25. S. M. Dhanasekaran *et al.*, *Nature* **412**, 822 (2001).
- S26. D. A. Wigle *et al.*, *Cancer Res* **62**, 3005 (2002).
- S27. T. R. Golub *et al.*, *Science* **286**, 531 (1999).
- S28. A. Rosenwald *et al.*, *Cancer Cell* **3**, 185 (2003).
- S29. C. Sotiropoulos *et al.*, *Proc Natl Acad Sci U S A* **100**, 10393 (2003).
- S30. E. Huang *et al.*, *Lancet* **361**, 1590 (2003).
- S31. D. J. Slamon *et al.*, *Science* **235**, 177 (1987).
- S32. D. R. Schwartz *et al.*, *Cancer Res* **62**, 4722 (2002).
- S33. A. A. Ferrando *et al.*, *Cancer Cell* **1**, 75 (2002).
- S34. X. Chen *et al.*, *Mol Biol Cell* **14**, 3208 (2003).
- S35. E. LaTulippe *et al.*, *Cancer Res* **62**, 4499 (2002).
- S36. S. Jain *et al.*, *Cancer Res* **64**, 3907 (2004).
- S37. A. A. Alizadeh *et al.*, *Nature* **403**, 503 (2000).
- S38. A. Rosenwald *et al.*, *N Engl J Med* **346**, 1937 (2002).
- S39. X. Chen *et al.*, *Mol Biol Cell* **13**, 1929 (2002).
- S40. U. Alon *et al.*, *Proc Natl Acad Sci U S A* **96**, 6745 (1999).
- S41. N. J. Lacayo *et al.*, *Blood* **104**, 2646 (2004).
- S42. G. V. Glinsky, A. B. Glinskii, A. J. Stephenson, R. M. Hoffman, W. L. Gerald, *J Clin Invest* **113**, 913 (2004).
- S43. T. O. Nielsen *et al.*, *Lancet* **359**, 1301 (2002).
- S44. A. J. Crew *et al.*, *Embo J* **14**, 2333 (1995).
- S45. Y. P. Yu *et al.*, *J Clin Oncol* **22**, 2790 (2004).